2,5-hexanedione induced apoptosis in mesenchymal stem cells from rat bone marrow via mitochondria-dependent caspase-3 pathway

Ruolin CHEN[1a], Shuang LIU[1a], Fengyuan PIAO[1]*, Zhemin WANG[1], Yuan QI[1], Shuangyue LI[1], Dongmei ZHANG[2] and Jingshun SHEN[3]*

[1]Department of Occupational and Environmental Health, Dalian Medical University, China
[2]Department of Physiology, Dalian Medical University, China
[3]Department of Neurology, First Affiliated Hospital of Dalian Medical University, China

Abstract: 2,5-hexanedione (HD) induces apoptosis of nerve cells. However,the mechanism of HD-induced apoptosis remains unknown. Mesenchymal stem cells (MSCs) are multipotential stem cells with the ability to differentiate into various cell types. This study is designed to investigate the apoptosis induced by HD in rat bone marrow MSCs (BMSCs) and the related underlying mechanisms. The fifth generation of MSCs was treated with 0, 10, 20 and 40 mM HD respectively. The viability of BMSCs was observed by MTT. Apoptosis were estimated by Hoechst 33342 staining and TUNEL assay. The disruption of mitochondrial transmembrane potential (MMP) was examined by JC-1 staining. Moreover, the expression of Bax and Bcl-2, cytochrome c release, and caspase-3 activity were determined by real-time RT-PCR, Western blot and Spectrophotometry. Our results showed that HD induced apoptosis in MSCs in a dose dependent manner. Moreover, HD down-regulated the Bcl-2 expression,upregulated the Bax expression and the Bax/Bcl-2 ratio, promoted the disruption of MMP, induced the release of cytochrome c from mitochondria to cytosol, and increased the activity of caspase-3 in MSCs. These results indicate that HD induces apoptosis in MSCs and the activated mitochondria-dependent caspase-3 pathway may be involved in the HD-induced apoptosis.

Key words: 2,5-hexanedione, Neurotoxicity, Mesenchymal stem cells, Apoptosis, Mitochondria-dependent caspase-3 pathway

Introduction

n-hexane is a kind of organic solvent and widely used in industrial processes including chemical engineering, pharmaceutical and cosmetic industry. Approximately 80–90% of n-hexane can be absorbed by inhalation and then is distributed to lipid-rich tissues and organs such as the brain, peripheral nerves, liver, spleen, kidneys and adrenal glands. The chemical is known to be a potent neurotoxicant and chronic exposure to it leads to severe neuropathy in humans and experimental animals[1, 2]. Metabolism studies have demonstrated that 2,5-hexanedione (HD), a metabolite of n-hexane, is the causative agent in n-hexane-induced neurotoxicity[1, 3]. Several studies showed that HD caused neuron loss. Ogawa *et al.*[4] evaluated effect of HD

---

on dorsal root ganglion cells from mice and discovered significant cell loss. Strange's study[5] found markedly reduced number and size of cultured neocortical neurons induced by HD. Zilz *et al.*[6] showed increase in apoptosis in the human neuroblastoma line SK-N-SH exposed to HD. Another research by us also showed that apoptosis in nerve tissue was significantly increased in rats exposed ton HD (Data no shown). These results indicated that HD exposure induces apoptosis of nerve cells. Kim *et al.*[3] reported that HD decreased viability of C17.2 cells as multipotent neural progenitor cells (NPC) isolated from neonatal mouse cerebellum and reduced numbers of newly generated cells in the hippocampus of mice. Moreover, it was indicated that the mechanism of apoptosis may be involved in HD-induced inhibition of NPC proliferation and hippocampal neurogenesis.

It is well known that mesenchymal stem cells (MSCs) are multipotential stem cells and have unique properties such as self-renewal, unlimited proliferation ability, plasticity to generate various cell types. Many studies have demonstrated that MSCs can directly differentiate into neurons and glial cells in vivo[7]. Moreover, it was proved that MSCs in vitro cultured can also spontaneously convert into nueral phenotype and carry with neural markers[8]. On the other hand, the characteristics of MSCs have been also concerned in the toxicity screening against chemical toxicants[9]. MSCs represent a good promise for the development of in vitro human and animal assays and could ultimately replace, improve or overtake current predictive models in toxicology. MSCs have been used as the model system for studies on effects of many chemicals including nerutoxicants on cell proliferation, survival and differentiation[10–12]. Recently, it was reported that some toxicants such as arsenic and lead can induce apoptosis of MSCs[13, 14]. Moreover, these studies have been widely concerned. Therefore, we are interested in whether HD induces apoptosis of MSCs and the possible mechanism of HD-induced apoptosis.

Mitochondria-dependent pathway is one of three different death signaling pathways leading to apoptosis[15, 16]. It has been documented that this pathway of apoptosis includes the disturbance in the expression of Bcl-2 family members, loss of mitochondrial transmembrane potential (MMP), release of cytochrome c from the mitochondria into the cytoplasm, activation of caspase-3 and ultimately trigger apoptosis[17, 18]. Bax and Bcl-2 are representative members of the Bcl-2 family. The former is proapoptotic molecule and the latter is antiapoptotic molecule. The two proteins are key mediators of cytochrome c release in the

context of apoptotic stimuli[19]. The release of cytochrome c is fundamental to apoptosome formation and downstream caspase-3 activation[20]. Caspase-3 is generally considered an important effector protease that is cleaved and activated during apoptosis[21]. Some researchers showed that HD exposure significantly altered expression of Bcl-2 and Bax, and activity of caspase-3 in nerve tissues of rats or human ovarian granulosa cells[22, 23]. These results indicate that the mitochondria-dependent pathway may be involved in HD-induced apoptosis.

In the present study, the viability and morphological alterations were observed in rat bone marrow MSCs (BMSCs) after treatment of 0, 10, 20 and 40 mM HD by MTT assay and HE staining. Apoptosis were estimated by Hoechst 33342 staining and TUNEL assay. MMP was examined through JC-1 staining. Moreover, we investigated the expression of Bax and Bcl-2, the release of cytochrome c and caspase-3 activity by real-time PCR, Western blotting and immunohistochemistry. The expression ratio of Bax/Bcl-2 proteins was also analyzed by statistical method. Our results suggested that HD exposure resulted in an increase in Bax and a decrease in Bcl-2, followed by loss of MMP, the release of cytochrome c and activation of caspase-3. These results indicate that HD induces apoptosis in the BMSCs via the activation of mitochondria-dependent caspase-3 signaling pathway. The study aimed at investigating the apoptotic effect of HD on the BMSCs and exploring its underlying mechanism of HD-induced apoptosis.

Materials and Methods

Animal care

All experiments were performed using Sprague-Dawley rats and were conducted according to the Dalian Medical University Guide for the Care and Use of Laboratory Animals. All experimental animal procedures were approved by the Animal Care and Use Committee of Dalian Medical University, Dalian, China.

Culture and differentiation of BMSCs

Isolation and expansion of BMSCs were performed according to a previously described protocol[24]. Male Sprague-Dawley rats (4 wk old) were euthanized and bone marrow was harvested by flushing femoral and tibial cavities with low-glucose Dulbecco's modified Eagle's medium (L-DMEM, Gibco BRL). Cells were passaged at a ratio of 1:3 plates when they reached approximately 90% confluence. BMSCs surface expression of CD29, CD45

and CD90 was analyzed by flow cytometry. The cells were cultured in adipogenic induced liquid, Then cells were stained with Oil red after three weeks; The cells cultured in osteogenesis induced liquid were identified by alizarin red staining after three weeks; The cells were cultured in Neuroblast induced liquid, and they were identified by immunocytochemical staining using neural specific enolase (NSE) antibody after 24, 48 and 72 h respectively.

Analysis of cell viability by MTT assay

Cell viability following HD (Sigma, St. Louis, MO, USA) exposure was examined using an HD, MTT (Sigma, St. Louis, MO, USA) assay. The fourth generation of rat BMSCs was seeded in 96-well plates at a density of 1×10^4 cells/ml. After incubation overnight, the medium was removed and the cells were incubated in 100 μl media supplemented with the concentrations of 0, 10, 20 and 40 mM HD for 12, 24 and 48 h respectively. At the end of treatment, 10 μl MTT solution (5 mg/ml in PBS) was added to each well and the cells further incubated in a 5% CO_2 humidified incubator at 37 °C for 4 h. The medium was then carefully removed, and the colored formazan was dissolved in 200 μl dimethyl sulfoxide (DMSO). The plate was shaken for 10 min and the absorbance was measured at 570 and 630 nm using a microplate reader (SPECTRA FLUOR, Austria). Cell viability was expressed as percent of the control culture value.

HE staining and Hoechst 33342 staining

The fourth generation of rat BMSCs was seeded into 24-well plates and allowed to attach for 24 h. Then cells were treated with 0, 10, 20 and 40 mM HD for 48 h. After various treatments, cells were washed with PBS twice for 5 min and fixed with 95% ethanol for 30 min. They were then washed with PBS twice for 5 min, stained with hematoxylin for 2 min and rinsed with running water. Clear nuclear staining was observed under the microscope, whereas non-staining was seen in the cytoplasm. The cells were then stained with 5% eosin for 2–3 min and rinsed with running water. Finally, they underwent open-air drying and were mounted in neutral resin. The morphological changes of cells were observed under optic microscopy (Olympus Optical Co., Ltd., Japan).

The fourth generation of rat BMSCs was seeded into 24-well plates. After various treatments as described above, cells were observed by microscope, and then fixed with 4% paraformaldehyde for 20 min at room temperature and washed with PBS thrice for 5 min. Cell nuclei were stained with Hoechst 33342 (Sigma, St. Louis, MO, USA)

at a final concentration of 10 mg/ml in PBS, for 20 min in a dark chamber. Then the cells were observed under converted fluorescence microscope (Olympus Optical Co., Ltd., Japan) and photographed.

Analysis of apoptosis by TUNEL assay

The TUNEL assay was performed using In Situ Cell Death Detection Kit and Fluorescein (Roche, Mannheim, Germany). All the procedures were based on manufacturer's protocol with slight modifications. In brief, cells cultured on 3.5 cm cell culture dishes were washed with PBS, fixed in 4% paraformaldehyde, washed with PBS again, and treated with permeabilization solution (0.1% Triton X-100 in 0.1% sodium citrate) for 2 min on ice. Afterward, the samples were then incubated with a terminal deoxynucleotidyl transferase (TdT) reaction mixture for 1 h at 37 °C in a humidified chamber, then stained with Hoechst 33342 (2 mg/ml in PBS) for 5 min. Finally, the samples were mounted with fluorescence mounting medium and visualized under confocal microscope (TCS SP5, Leica, Mannheim, Germany).

Quantitative real-time PCR and Western blotting

Total RNA was extracted from the fifth generation of rat BMSCs by using RNAisoPlus according to the manufacturer's instructions (Takara, Japan). The RNA was quantified by using a spectrophotometer. Only RNA samples with an A260/A280 of 1.8–2.2 were used for reverse transcription. 100 ng/μl of total RNA was reverse-transcribed using Reverse Transcription Kit (Takara, Japan). Quantitative real-time PCR was carried out with SYBR Green II PCR kit (Takara, Japan) using a TP800 Real-Time PCR Detection System (Takara, Japan). The primers for Bax, Bcl-2 and β-actin are shown in Table 1 (designed by Takara, Dalian). The reaction conditions were as follows: an initial denaturation at 95 °C for 5 min, followed by 40 cycles of 95 °C for 30 s, 55 °C for 30 s and 72 °C for 30 s. The β-actin mRNA was used as internal control probe.

Table 1. Specific primer sequences used in RT-PCR

Gene	Primer
Bax	FR: 5'-CGAATTGGCGATGAACTGGA-3'
	RP: 5'-CAAACATGTCAGCTGCCACAC-3'
Bcl-2	FR: 5'-GACTGAGTACCTGAACCGGCATC-3'
	RP: 5'- CTGAGCAGCGTCTTCAGAGACA-3'
β-actin	FR: 5'-GGAGATTACTGCCCTGGCTCCTA-3'
	RP: 5'-GACTCATCGTACTCCTGCTTGCTG-3'

The fifth generation of rat BMSCs was homogenized in ice-cold RIPA Tissue Protein Extraction Reagent (Biyuntian, China) supplemented with 1% proteinase inhibitor mix and incubated at 4 °C for 1 h. After incubation, debris was removed by centrifugation at 14,000 × g for 15 min at 4 °C and the lysates were stored at −80 °C until used. The total protein concentration in the lysates was determined using the BCA protein assay kit (Biyuntian, China). The proteins (50 μg/lane) were mixed with an equal volume of SDS-PAGE loading buffer and separated by SDS-PAGE under no-reducing conditions using 10% SDS-PAGE Gels and then electrotransferred to Hybond-P PVDF membrane (Millipore, France). The membrane was blocked with blocking buffer containing defatted milk power for 1 h and incubated overnight at 4 °C with rabbit anti-rat Bcl-2 Polyclonal antibody (1:400) (Cell Signaling Technology, USA) and rabbit anti-rat Bax Polyclonal antibody (1:400) (Cell Signaling Technology, USA). The membrane was washed three times with Tris buffered saline containing 0.05% Tween-20 (TBST) for 10 min and then incubated at room temperature for 1 h with horseradish peroxidase-conjugated goat anti-rabbit IgG (1:4000) (Sigma, USA) and horseradish peroxidase-conjugated goat anti-rabbit IgG (1:4000) (Sigma, USA). The signals were visualized using an enhanced ECL chemoluminescence kit and quantified densitometrically using UVP BioSpectrum Multispectral Imaging System (Ultra-Violet Products Ltd. Upland, CA, USA).

Detection of MMP using JC-1 and Determination of cytochrome c protein expression

The impact of HD on MMP in BMSCs was measured by histochemical staining using the sensitive and relatively mitochondrion-specific lipophilic cationic probe fluorochrome JC-1. JC-1 accumulates to form J-aggregates and emits red fluorescence in the mitochondria of higher membrane potentials, yet dissociates into monomers and emits green fluorescence in those that lose cross-membrane electrochemical gradient. The ratio of red to green fluorescence therefore provides a reliable estimate of impairment of MMP. For this assay, BMSCs washed with PBS were first examined under a fluorescence microscope to measure the baseline intensity of fluorescence from the inherent red color of HD. Cells were then incubated with JC-1 (5 μmol/L) in L-DMEM at 37 °C for 20 min and analyzed with confocal microscope (TCS SP5, Leica, Mannheim, Germany) and Image-Pro Plus 6.0 (Labsystems, MA, USA) to determine the ratio of green (excitation/emission wavelength=485/538 nm) to red (excitation/ emission wavelength=485/590 nm) fluorescence, both normalized to baseline value.

Preparation of cytosolic fractions was achieved using acommercially available cytosol/mitochondria fractionation kit according to the manufacturer's protocol (Beyotime, China). Cellular proteins were extracted with T-PER (Pierce Biotechnology, Inc., Rockford, IL, USA) and centrifuged at 12,000 rpm for 20 min. Protein concentrations were determined using the Bradford protein assay with bovine serum albumin (BSA) as a standard. Protein samples were stored at −80 °C until used. The total protein concentration in the lysates was determined using the BCA protein assay kit (Biyuntian, China). The proteins (50 μg/lane) were mixed with an equal volume of SDS-PAGE loading buffer and separated by SDS-PAGE under no-reducing conditions using 10% SDS-PAGE Gels and then electrotransferred to Hybond-P PVDF membrane (Millipore, France). The membrane was blocked with blocking buffer containing defatted milk power for 1 h and incubated overnight at 4 °C with rabbit anti-rat cytochrome c Polyclonal antibody (1:100) (Biyuntian, China). The membrane was washed three times with Tris buffered saline containing 0.05% Tween-20 (TBST) for 10 min and then incubated at room temperature for 1 h with horseradish peroxidase-conjugated goat anti-rabbit IgG (1:4000) (Sigma, USA) and horseradish peroxidase-conjugated goat anti-rabbit IgG (1:4000) (Sigma, USA). The signals were visualized using an enhanced ECL chemoluminescence kit and quantified densitometrically using UVP BioSpectrum Multispectral Imaging System (Ultra-Violet Products Ltd. Upland, CA, USA).

Determination of caspase-3 activity

The activity of caspase-3 was determined using the Caspase-3 activity kit (Beyotime Institute of Biotechnology, Haimen, China). To evaluate the activity of caspase-3, cell lysates were prepared after their respective treatment with various designated treatments. Assays were performed on 96-well microtitre plates by incubating 40 μl protein of cell lysate per sample in 50 μl reaction buffer (1% NP-40, 20 mM Tris-HCl (pH 7.5), 137 mM Nad and 10% glycerol) containing 10 µl caspase-3 substrate (Ac-DEVDpNA) (2 mM). Lysates were incubated at 37 °C for 2 h. Samples were measured with a microplate reader (SPECTRA FLUOR, Austria) at an absorbance of 405 nm and it represented the caspase-3 activity of this sample.

Statistical analysis

Data were presented as mean ± standard deviation (SD) from at least three independent experiments. All data
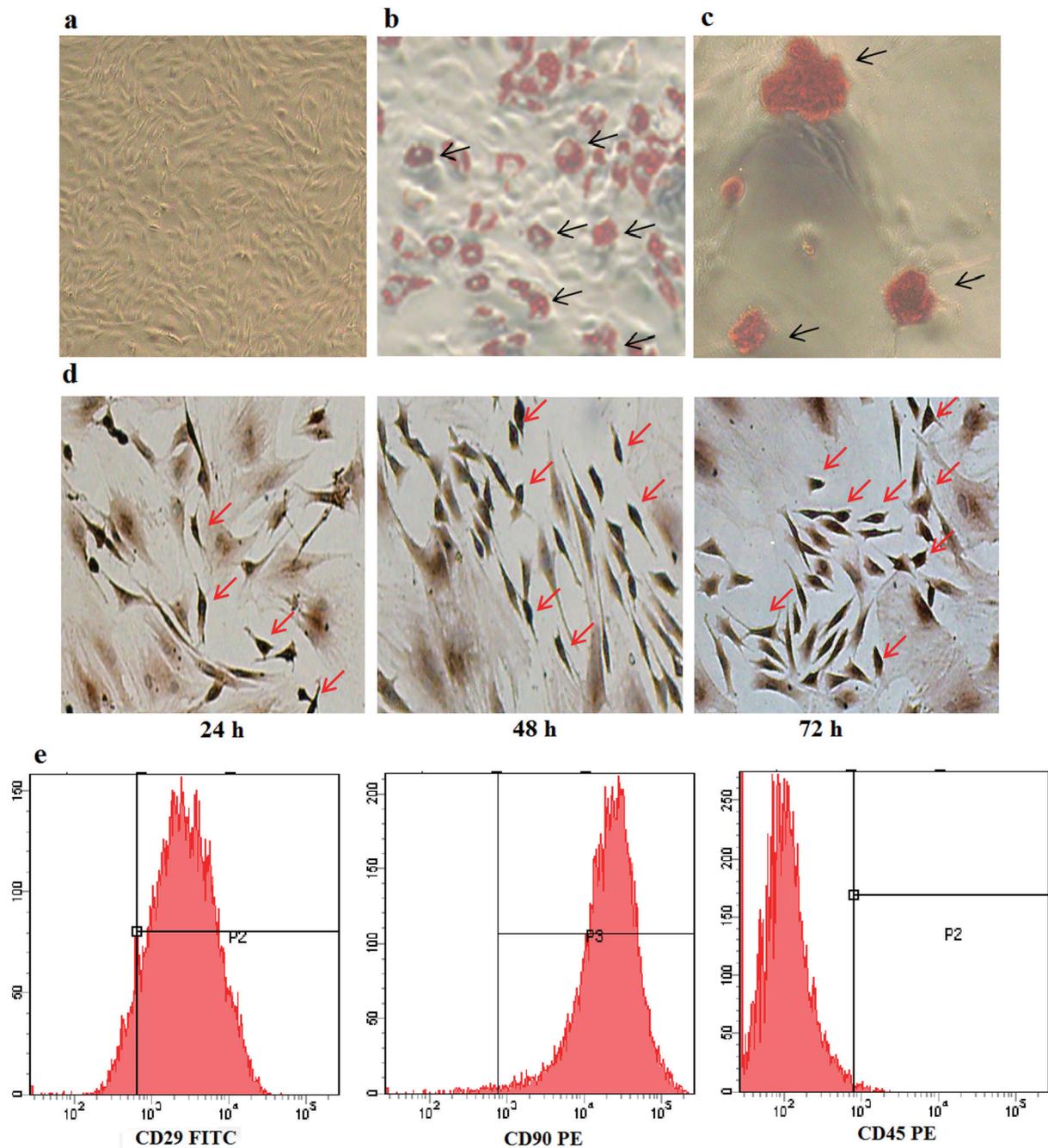
Fig. 1. Morphology and qualification of BMSCs. Morphology and qualification of BMSCs were assessed by optic microscopy and flow cytometry. a: Morphology observation of the 5th generation BMSCs. b: Adipogenic induction using Oil red O staining. c: Osteogenous induction using alizarin red calcification nodule staining. d: Cells were cultured in Neuroblast induced liquid at 24, 48 and 72 h, respectively. Then the expression of NSE antibody was detected by immunocytochemistry. e: Expression of CD29,CD90 and CD45 as surface markets was determined using flow cytometry.

were analyzed with SPSS 13.0 for windows. Difference in mean values between groups was tested with the one-way ANOVA and LSD test. *P* values less than 0.05 were considered significant.

Results

Morphology and qualification of BMSCs

The morphology of the BMSCs showed spindle-like or spindle-shaped and was almost uniform (Fig. 1a). Pheno-

typic cell surface markers of the BMSCs were determined using flow cytometry. The expression of CD29, CD90 and CD45 was 90.10%, 96.61% and 0.40%, respectively (Fig. 1e). After induction, a strong reaction was observed in the BMSCs by oil red O staining and alizarin red staining (Fig. 1b, c). It was indicated that BMSCs were differentiated into osteoblasts and adipocytes. Expression of NSE was analyzed in the cells cultured in Neuroblast induced liquid. The results showed 29.26%, 33.95% and 51.86% after 24, 48 and 72 h respectively (Fig. 1d), while the control group was negative for their marker. It was indicated that BMSCs were differentiated into nerve cells. These results revealed that the cultivated cells were BMSCs rather than hematopoietic cells or their progenitors.

Effects of HD on viability of BMSCs

Viability of BMSCs in the groups was shown in Fig. 2. There were no significant differences in viability of BMSCs between the experimental groups and control group at 12 h after HD exposure ($p>0.05$). However, viability of BMSCs in the exposed groups at 24 and 48 h was significantly lower than that in control group ($p<0.05$) and decreased in a dose-dependent manner. The results indicated that HD had cytotoxic effects on BMSCs.

Effect of HD on the morphology of BMSCs

The morphological changes of BMSCs stained by HE were shown in Fig. 3a. Our results showed that BMSCs in the control group showed fusiform or polygonal morphology and had ovoid nuclei. The cytoplasm was uniform staining. However, the BMSCs with pyknotic and darkly stained nuclei were observed in groups exposed to HD. Moreover, the cytoplasm dissolved and the polygonal apophysis became shoter or disappeared (Fig. 3a).

Apoptotic effect of HD on BMSCs

The morphological phenotype of the HD-treated BMSCs stained by Hoechst 33342 was shown in Fig. 3b. The results showed that the nuclei of control BMSCs were of a rounded shape with homogeneous intensity. However, the HD-exposed BMSCs showed crescent-shaped nuclei and fragmentation with heterogeneous intensity in the nuclei, suggesting that these cells underwent gross morphological change indicative of apoptosis (Fig. 3b).

Apoptotic cells in BMSCs stained by TUNEL are shown in Fig. 4. The TUNEL-positive neuronal cells were found in the BMSCs exposed to HD (Fig. 4a). However, the TUNEL-positive cells were almost absent in the BMSCs of control group. The results of apoptotic index showed
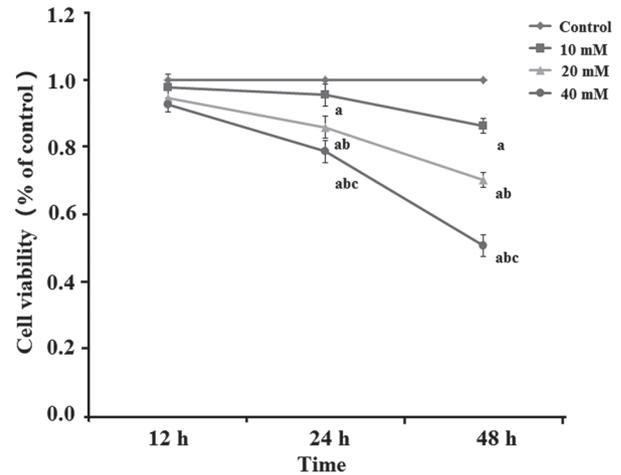

Fig. 2. Effect of HD on viability of BMSCs. BMSCs were treated with 0, 10, 20 and 40 mM HD for 12, 24 and 48 h, respectively. Cell viability was assayed by MTT analysis. Data are presented as mean ± SD from three independent experiments. a: $p<0.05$, compared with control group; b: $p<0.05$, compared with 10 mM group; c: $p< 0.05$, compared with 20 mM group.

that the TUNEL-positive neuronal cells were significantly higher in the BMSCs exposed to HD than those in control group ($p<0.05$) and increased in a dose-dependent manner (Fig. 4b).

Effect of HD on expression of Bcl-2 and Bax in BMSCs

The mRNA expression of Bax and Bcl-2 in BMSCs exposed to 0, 10, 20 and 40 mM HD is shown in Fig. 5a and 5b. The mRNA expression of Bax in BMSCs was significantly higher in the groups receiving HD than that in control group ($p<0.05$). Moreover, the mRNA expression of Bax in BMSCs exposed to HD increased in a dose-dependent manner. On the other hand, the mRNA expression of Bcl-2 in BMSCs exposed to HD was significantly lower than that in control group ($p<0.05$). Because an alteration in the ratio of Bax/Bcl-2 is a more sensitive and reliable marker than individual Bax and Bcl-2 levels, the expression ratio of Bax/Bcl-2 genes in the BMSCs was also analyzed. The ratio of Bax/Bcl-2 gene expression in the treated BMSCs significantly increased in the experimental groups compared with the control group ($p<0.05$). Especially, the ratio of Bax/Bcl-2 gene expression in the BMSCs exposed to 40 mM HD was the highest among the 4 groups (Fig. 5c).

The expression of Bax and Bcl-2 proteins in the BMSCs by Western blot is shown in Fig. 5d and 5e. The expression of Bax protein in the BMSCs was significantly higher in the groups receiving HD than that in control group
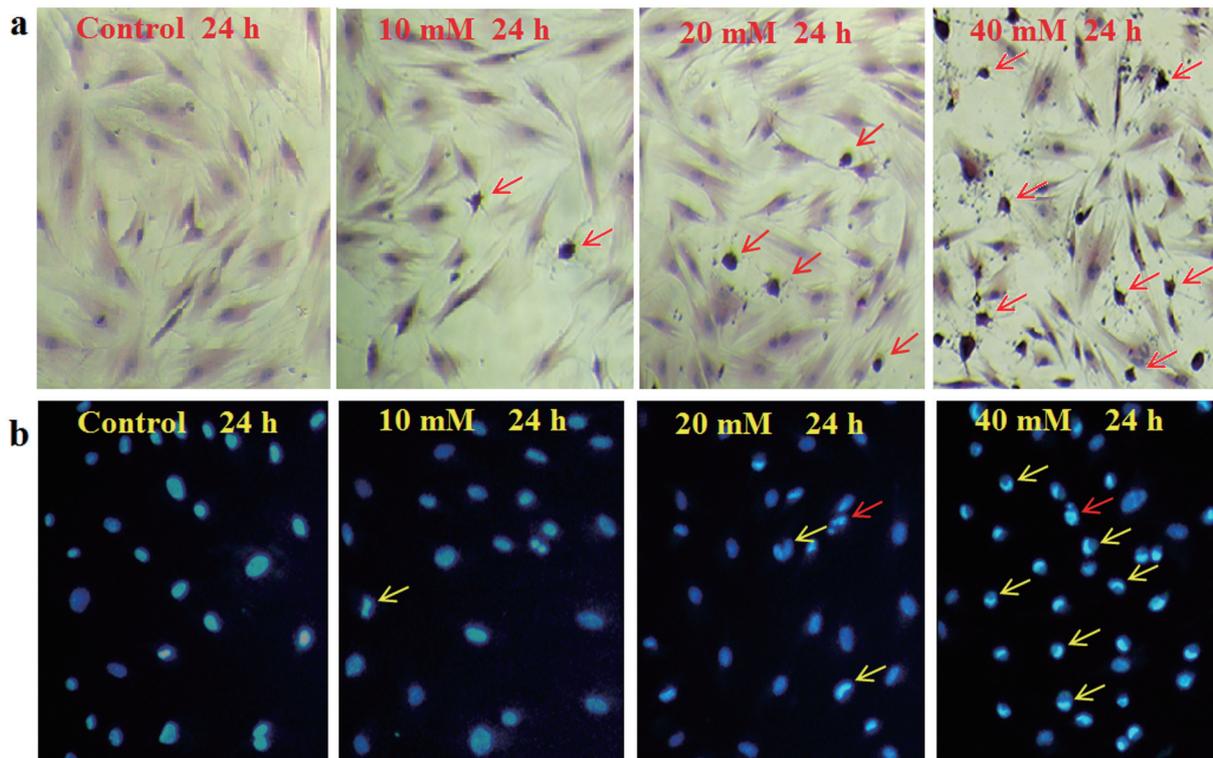
Fig. 3.   The morphology of BMSCs exposed to HD. BMSCs were treated with 0, 10, 20 and 40 mM HD for 24 h. a: Cell morphological changes were observed with optic microscopy after HE staining. Arrows indicated the BMSCs with pyknotic and darkly stained nuclei. The images are representative for three independent experiments. b: Apoptosis was observed with fluorescence microscopy after nuclei staining with Hoechst 33342. Yellow arrows indicated apoptotic cells with crescent-shaped nuclei; Red arrows indicated apoptosis cells with fragmentary nuclei. The images are representative for three independent experiments.

($p<0.05$). However, the expression of Bcl-2 protein in the BMSCs exposed to HD was significantly lower than that in controls ($p<0.05$). The ratio of Bax/Bcl-2 protein expression in the BMSCs significantly increased in the experimental groups compared with the control group ($p<0.05$) (Fig. 5f).

Effect of HD on mitochondrial membrane potential in BMSCs

The mitochondrial potential sensor JC-1 was used to determine the mitochondria function (Fig. 6a). It forms J-aggregates in intact mitochondria that result in emission of red/green fluorescence, whereas it forms monomers upon the mitochondrial membrane depolarization that emit green fluorescence. As shown in Fig. 6b, the ratio of red to green fluorescence was $90.9 \pm 0.2\%$ in control group and $30.3 \pm 0.6\%$, $13.9 \pm 0.3\%$ and $7.1 \pm 0.5\%$ in the groups exposed to 10, 20 and 40 mM HD, respectively. The ratio of red to green fluorescence in the experimental groups was significantly higher than that in control group ($p<0.05$). The decreased ratio of red to green fluorescence suggests

that HD induces MMP depolarization in the BMSCs.

Effect of HD on protein expression of cytochrome c in BMSCs

The expression of cytochrome c protein was evaluated by western blot in BMSCs treated with HD. The results showed that expression level of cytochrome c protein in mitochondria was significantly lower in the BMSCs receiving HD than that in control group ($p<0.05$). Moreover, the expression of cytochrome c protein in mitochondria of the BMSCs exposed to HD increased in a dose-dependent manner (Fig. 6c). On the other hand, expression of cytochrome c protein in cytosol was significantly higher in the BMSCs receiving HD than that in control group ($p<0.05$) and decreased in a dose-dependent manner (Fig. 6d).

Effects of HD on caspase-3 activation in BMSCs

Activity of caspase-3 in BMSCs exposed to 0, 10, 20 and 40 mM HD is shown in Fig. 7. The activity of caspase-3 in BMSCs was significantly higher in the groups receiving HD than that in control group ($p<0.05$).
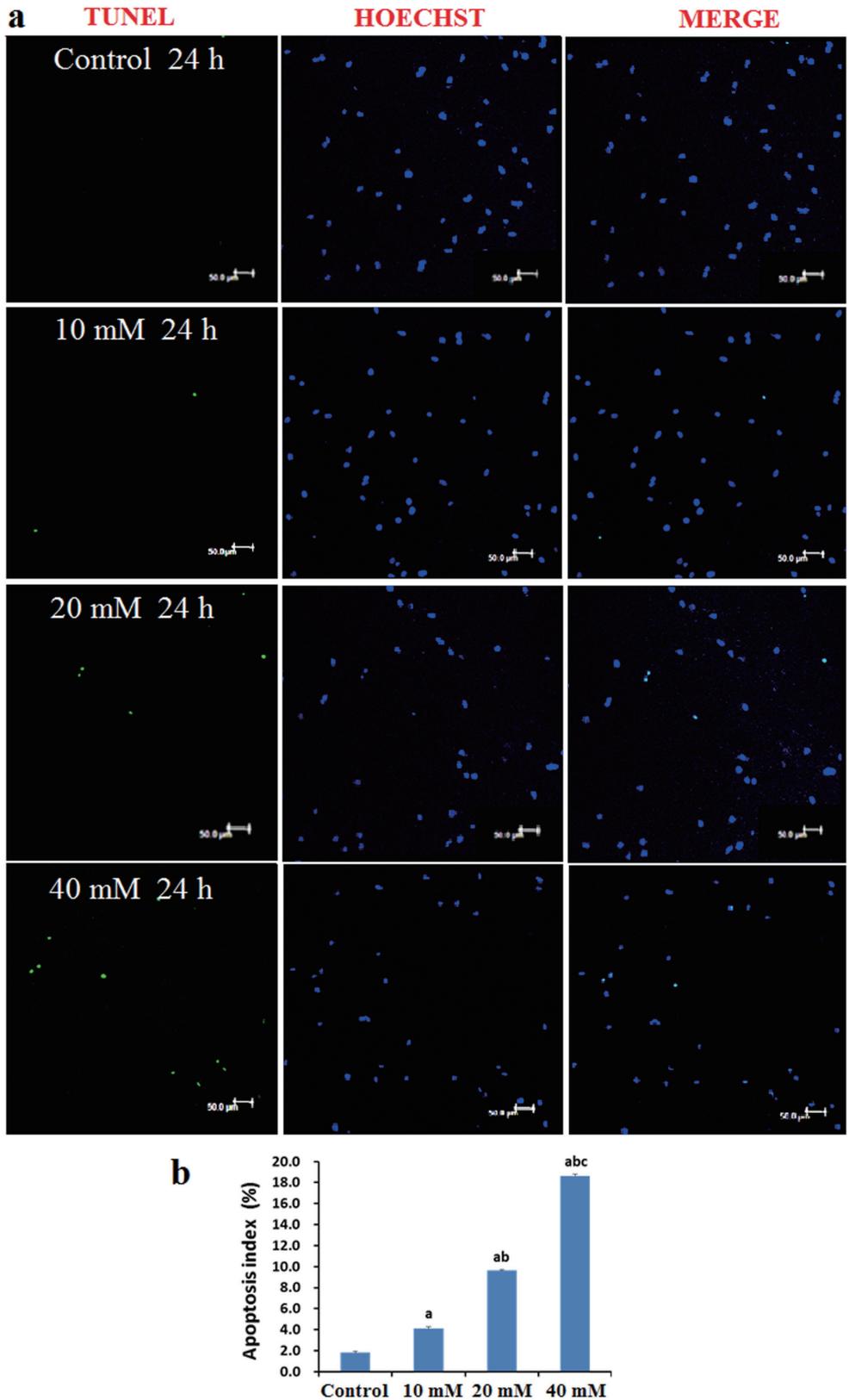
Fig. 4.   Apoptosis in BMSCs exposed to HD. BMSCs were treated with 0, 10, 20 and 40 mM HD for 24 h. a: Apoptosis in BM-SCs was observed by TUNEL assay. Green color represents TUNEL-positive cells as apoptosis. Blue color represents cell nuclei counterstained with Hoechst 33342. Scale bar=50 μm. b: Data are presented as mean ± SD from three independent experiments. a: $p < 0.05$, compared with control group; b: $p < 0.05$, compared with 10 mM group; c: $p < 0.05$, compared with 20 mM group.
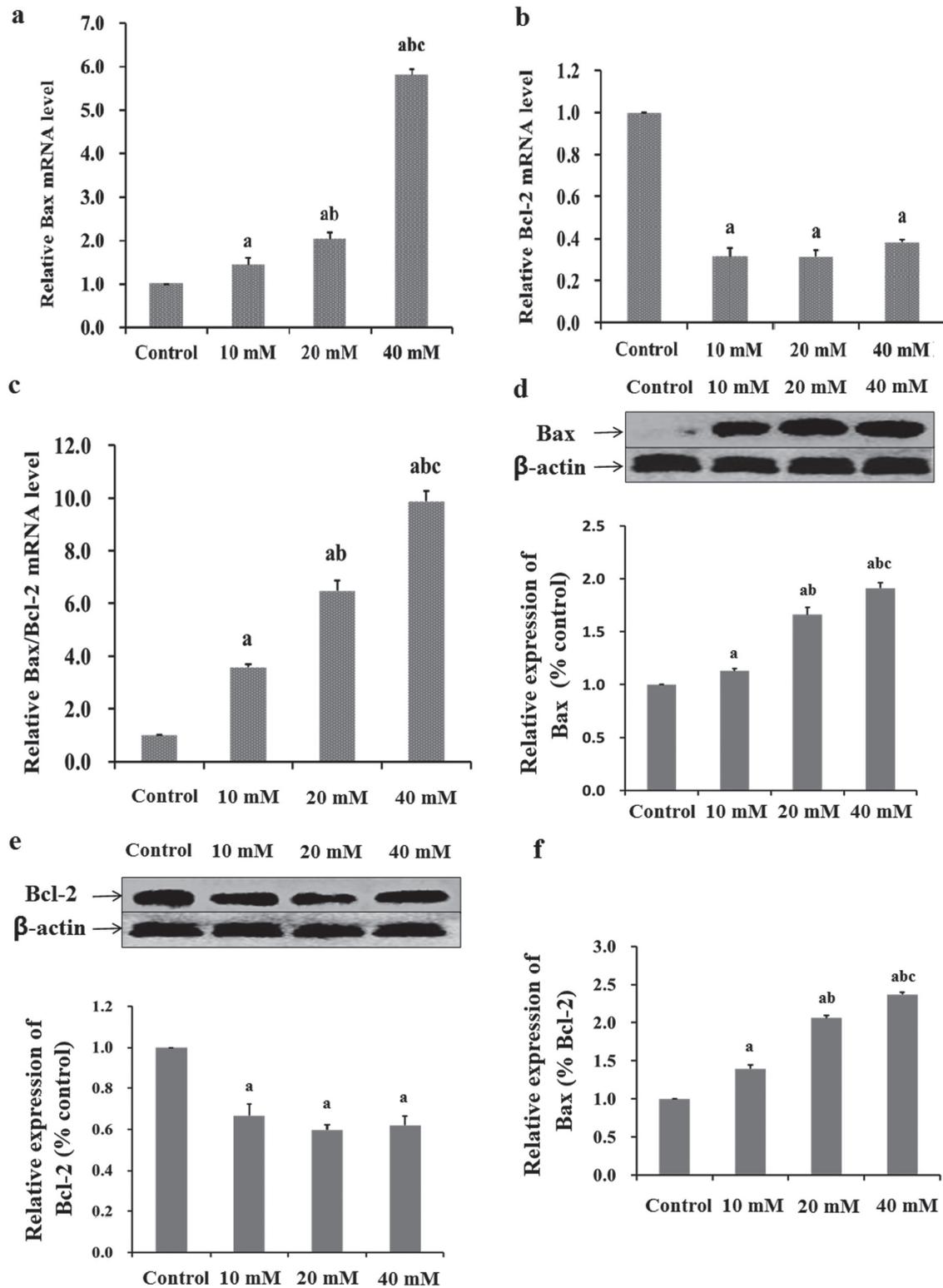
Fig. 5. Expression of Bax and Bcl-2 in BMSCs exposed to HD. BMSCs were treated with 0, 10, 20 and 40 mMHD for 24 h. Real-time quantitative PCR was used to detect Bax and Bcl-2 mRNA expression; Western blot analysis was used to detect Bcl-2 and Bax protein expression. a: Bax mRNA expression in BMSCs exposed to HD. b: Bcl-2 mRNA expression in BMSCs exposed to HD. c: The ratio of Bax/Bcl-2 mRNA expression in BMSCs exposed to HD. d: Bax protein expression in BMSCs exposed to HD. e: Bcl-2 protein expression in BMSCs exposed to HD. f: The ratio of Bax/Bcl-2 protein expression in BMSCs exposed to HD. Data are presented as mean ± SD from three independent experiments. a: $p<0.05$, compared with control group, b: $p<0.05$, compared with 10 mM group, c: $p<0.05$, compared with 20 mM group.
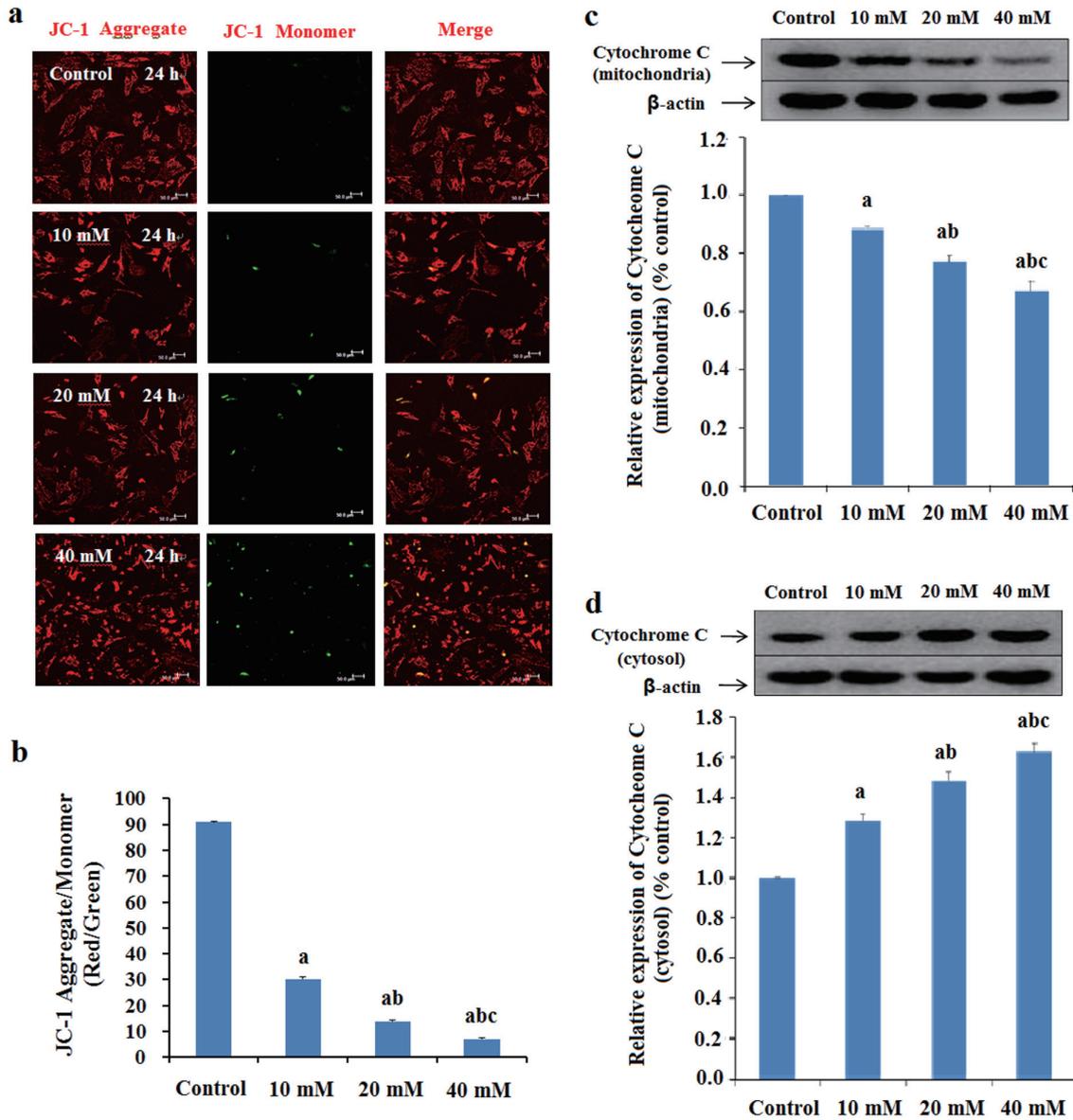
Fig. 6.   The loss of MMP and Cytochrome C protein expression in BMSCs exposed to HD. BMSCs were treated with 0, 10, 20 and 40 mM HD for 24 h. The confocal images of the MMP loss were shown by JC-1 fluorescence. Western blot analysis was used to detect Cytochrome C protein level. a: Red fluorescence represents the mitochondrial aggregate JC-1 and green fluorescence indicates the monomeric JC-1, Scale bar=50 μm. b: Expression of cytochrome c in the mitochondrial fraction in BMSCs exposed to HD. c: Expression of cytochrome c in the cytosolic fraction in BMSCs exposed to HD. d: Data are presented as mean ± SD from three independent experiments. a: $p<0.05$, compared with control group; b: $p<0.05$, compared with 10 mM group; c: $p<0.05$, compared with 20 mM group.

Especially,the caspase-3 activity was the highest in BMSCs exposed to 40 mM HD among the four groups.

Discussion

Many studies have documented that HD is the causative agent in n-hexane-induced neurotoxicity. Although some hypotheses have been proposed[25, 26], the mechanism of HD-induced neurotoxicity is still not completely understood. The researches indicated that an abnormal increase in apoptosis is the main form of cell death caused by certain injuries[23, 27]. Sun et al.[23] reported that HD can cause granulosa cell apoptosis. Moreover, it was reported that apoptosis may be one of the mechanisms by which HD induces cell death. In the present study, viability and apoptosis were observed in the BMSCs exposed to 0, 10,
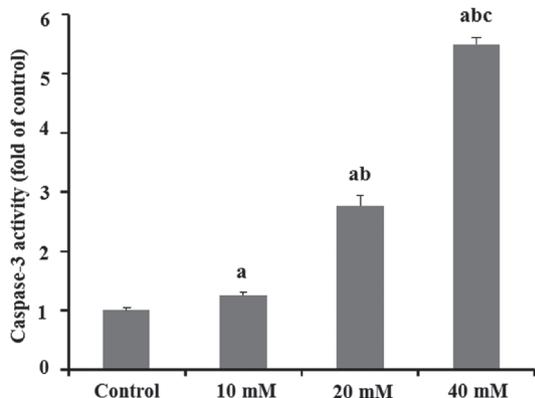
Fig. 7. Caspase-3 activity in BMSCs exposed to HD. BM-SCs were treated with 0, 10, 20 and 40 mM HD for 24 h. Data are presented as mean ± SD from three independent experiments. a: *p*<0.05, compared with control group; b: *p*<0.05, compared with 10 mM group; c: *p*<0.05, compared with 20 mM group.

20 and 40 mM HD by the MTT, Hoechst and TUNEL assays. We found that survival BMSCs cells decreased as dose-dependence after HD exposure and that apoptosis cells increased as dose-dependence, which suggested that the decreased survival cells were caused by the apoptotic effect of HD. Our results were accordance to the studies in above. These results indicate that HD exposure may induce apoptosis in BMSCs and the mechanism of apoptosis may be involved in HD-induced neurotoxicity.

Apoptosis is tightly regulated by antiapoptotic and proapoptotic effector molecules, including proteins of the Bcl-2 family[28]. It is well-known that Bax and Bcl-2 are representative members of this family and Bax promotes apoptosis, while Bcl-2 plays a role in preventing apoptosis[29]. Cui *et al.*[22] showed that HD significantly altered expression of Bax and Bcl-2 in nerve tissues of rats. Sun *et al.*[23] reported that with increasing HD doses, the expression of Bcl-2 decreased and the expression of Bax increased in human ovarian granulosa cells. In the present study, we examined mRNA and protein expression levels of Bax and Bcl-2 in HD-exposed MSCs. Our results showed that the expression of Bax gene and its protein was significantly higher in the BMSCs exposed to HD that in control group and increased in dose dependant manner. On the other hand, the expression of Bcl-2 gene and its protein was significantly lower in the BMSCs exposed to HD that in control group. Our findings corresponded with the decreased viability and the increased apoptosis in the HD-exposed BMSCs and were consistent with the results in above. It has been indicated that the ratio of Bax to Bcl-

2 is an important determinant of cellular susceptibility to apoptosis and could ultimately tip the balance toward cell survival or cell death[30]. Accordingly, the ratio of Bax/Bcl-2 is frequently used to evaluate the occurrence of apoptosis[29]. Our results showed that the expression ratio of Bax/Bcl-2 genes or proteins in the BMSCs exposed to HD significantly increased in the experimental groups compared with the control group (*p*<0.05). It was reported that some inducers of apoptosis including arsenic and lead can significantly increase the ratio of Bax/Bcl-2 in the treated animal models, supporting our results[14, 31]. These results indicate that HD downregulates Bcl-2 expression and upregulates Bax expression, and the expression ratio of Bax/Bcl-2 in the HD-exposed BMSCs. It is also suggested that HD may induce apoptosis in the BMSCs via disturbing balance in Bax/Bcl-2 expression.

Mitochondrial apoptosis pathway is thought to be the intrinsic apoptotic pathway and plays a vital role to the neuron apoptosis. It was reported that the increased ratio of Bax/Bcl-2 leads to MMP disruption and cytochrome c release, which in turn activates the caspase cascade[32]. Moreover, it was shown that disruption of MMP is one of the earliest intracellular events that occur during the initial phase of apoptosis via the mitochondria-mediated death pathway[33]. Lots of evidences indicated that the loss of MMP was associated with the apoptosis induced by some toxicants[34, 35]. It was reported that HD exposure induced the loss of MMP in rat spermatogenic cells[36]. In the present study, a significant decrease in MMP was also observed in HD-exposed BMSCs in a dose-dependent manner, being consistent with the above results. Several reports have suggested that the loss of MMP eventually causes the efflux of death-promoting cytochrome c from mitochondria to cytosol. We also found an increase of cytochrome c in cytosolic fraction and a corresponding decrease in mitochondrial fraction in the BMSCs after HD exposure. Our results indicate that HD exposure induces the loss of MMP and translocation of cytochrome c in the BMSCs. It is also suggested that the reduced MMP and the released cytochrome c may be involved in the activation of caspase cascade in the BMSCs exposed to HD.

Caspase activation is an indispensable event in the initiation of mitochondria-mediated apoptosis[37]. Among the identified caspases, caspase 3 is thought to be the key enzyme that induces apoptosis. It is the ultimate enforcer of caspases in apoptosis. Its activation, a downstream key step to execute apoptosis[38], has been demonstrated in various cells undergoing mitochondria-mediated apoptosis[23, 35, 39–41]. It was reported that an increase in the active

caspase 3 expression was shown in HD-exposed human ovarian granulosa cells[23]. Mishra *et al.*[36] found that HD caused the activation of caspase 3 in spermatogenic cells. In this study, the results showed that activity of caspase 3 was significantly increased by HD in a dose-dependent manner, being consistent with those results in above. Our results indicate that HD exposure upregulates activity of caspase 3 in the BMSCs. It is also suggested that the activated caspase 3 may triggered the HD-induced apoptosis in the BMSCs.

In vitro cytotoxicity tests are typically carried out with transformed, immortalized cell lines or primary cells. Because the transformed and immortalized cell lines were obtained from cancerous tissues carrying mutated genes or chromosomal instability which is directly involved in cell cycle kinetics, cell death pathways or drug detoxification, the genetic background of these cells may complicate the analyses of cytotoxicity related cell signaling pathways. Primary cells are considered a better option as model systems for predicting toxicological behavior, however they are limited in quantity and suffer from batch-to-batch variation due to the need to isolate them freshly for each study. It is recognized that stem cells have many advantages over primary cells and transformed or immortalized cell lines for in vitro toxicity screening, including unique properties such as unlimited self-renewal, plasticity to generate various cell types, and availability of cells of human origin[41, 42]. Moreover, MSCs can provide a much cleaner system and the untransformed culture should theoretically provide more accurate modeling of in vivo condition, ensuring that the results are more comparable to in vivo effects. Moreover, this model may allow prediction of cytotoxicity at both the developmental and mature stages. Therefore, MSCs represent a good promise for the development of in vitro human and animal assays. MSCs are one of the representative adult stem cells and has a differentiation potential into multilineages including neurogenic and hepatogenic lineages[43]. Hence, the characteristics of MSCs are attentive in the toxicity screening against chemical toxicants. Cai *et al.*[31] reported that arsenic trioxide induced the apoptosis of BMSCs from rat and increased the caspase-3 activity. Sharifi *et al.*[14] found that lead acetate induced apoptosis in a dose-dependent manner in rat BMSCs and over-expression of pro-apoptotic proteins including Bax and caspases-3. In the present study, our results showed HD induced apoptosis in MSCs via activating the intrinsic apoptotic pathway, being accordant with the results in above. Our results will provide experimental evidence for applying in vitro MSCs to examine toxicities of chemical toxicants including induction of apoptosis.

In conclusion, the present study showed that HD exposure induced the decreased viability, abnormal morphological changes and apoptosis in the BMSCs. The expression of Bax was upregulated, the expression of Bcl-2 was downregulated and expression ratio of Bax/Bcl-2 was increased in the BMSCs exposed to HD. Moreover, HD caused the loss of MMP, cytochrome c release from mitochondria to the cytosol and caspase-3 activation in the BMSCs. Our results indicate that HD induces apoptosis in the BMSCs via the activation of mitochondria-dependent caspase-3 signaling pathway. These results may provide the research clue and reference for further exploring the mechanism of HD-induced neurotoxicity. However, further studies are still needed to clarify the precise molecular mechanism of HD-induced neurotoxicity in vivo.

Acknowledgements

References

1) Neghab M, Soleimani E, Khamoushian K (2012) Electrophysiological studies of shoemakers exposed to sub-TLV levels of n-hexane. J Occup Health **54**, 376–82.

2) Rao DB, Jortner BS, Sills RC (2014) Animal models of peripheral neuropathy due to environmental toxicants. ILAR J **54**, 315–23.

3) Kim MS, Park HR, Park M, Kim SJ, Kwon M, Yu BP, Chung HY, Kim HS, Kwack SJ, Kang TS, Kim SH, Lee J (2009) Neurotoxic effect of 2,5-hexanedione on neural progenitor cells and hippocampal neurogenesis. Toxicology **260**, 97–103.

4) Ogawa Y, Shimizu H, Kim SU (1996) 2,5-Hexanedione induced apoptosis in cultured mouse DRG neurons. Int Arch Occup Environ Health **68**, 495–7.

5) Strange P, Møller A, Ladefoged O, Lam HR, Larsen JJ, Arlien-Søborg P (1991) Total number and mean cell volume of neocortical neurons in rats exposed to 2,5-hexanedione with and without acetone. Neurotoxicol Teratol **13**, 401–6.

6) Zilz TR, Griffiths HR, Coleman MD (2007) Apoptotic and necrotic effects of hexanedione derivatives on the human neuroblastoma line SK-N-SH. Toxicology **231**, 210–4.

7) Steiner JP, Nath A (2014) Neurotrophin strategies for neuroprotection: are they sufficient? J Neuroimmune Pharmacol **9**, 182–94.

8) Moradi F, Haji Ghasem Kashani M, Ghorbanian MT, Lashkarbolouki T (2012) Spontaneous expression of

neurotrophic factors and TH, Nurr1, Nestin Genes in Long-term Culture of Bone Marrow Mesenchymal Stem Cells. Cell J **13**, 243–50.

9) Scanu M, Mancuso L, Cao G (2011) Evaluation of the use of human mesenchymal stem cells for acute toxicity tests. Toxicol In Vitro **25**, 1989–95.

10) Despang F, Bernhardt A, Lode A, Hanke T, Handtrack D, Kieback B, Gelinsky M (2010) Response of human bone marrow stromal cells to a novel ultra-fine-grained and dispersion-strengthened titanium-based material. Acta Biomater **6**, 1006–13.

11) Podechard N, Fardel O, Corolleur M, Bernard M, Lecureur V (2009) Inhibition of human mesenchymal stem cell-derived adipogenesis by the environmental contaminant benzo(a)pyrene. Toxicol In Vitro **23**, 1139–44.

12) Szewczyk L, Ulańska J, Dubiel M, Osyczka AM, Tylko G (2012) The effect of acrylamide and nitric oxide donors on human mesenchymal progenitor cells. Toxicol In Vitro **26**, 897–906.

13) Yadav S, Shi Y, Wang F, Wang H (2010) Arsenite induces apoptosis in human mesenchymal stem cells by altering Bcl-2 family proteins and by activating intrinsic pathway. Toxicol Appl Pharmacol **244**, 263–72.

14) Sharifi AM, Ghazanfari R, Tekiyehmaroof N, Sharifi MA (2011) Investigating the effect of lead acetate on rat bone marrow-derived mesenchymal stem cells toxicity: role of apoptosis. Toxicol Mech Methods **21**, 225–30.

15) Shen Y, Luo Q, Xu H, Gong F, Zhou X, Sun Y, Wu X, Liu W, Zeng G, Tan N, Xu Q (2011) Mitochondria-dependent apoptosis of activated T lymphocytes induced by astin C, a plant cyclopeptide, for preventing murine experimental colitis. Biochem Pharmacol **82**, 260–8.

16) Zuo H, Lin T, Wang D, Peng R, Wang S, Gao Y, Xu X, Li Y, Wang S, Zhao L, Wang L, Zhou H (2014) Neural cell apoptosis induced by microwave exposure through mitochondria-dependent caspase-3 pathway. Int J Med Sci **11**, 426–35.

17) Hsia TC, Yu CC, Hsu SC, Tang NY, Lu HF, Huang YP, Wu SH, Lin JG, Chung JG (2014) Cantharidin induces apoptosis of H460 human lung cancer cells through mitochondria-dependent pathways. Int J Oncol **45**, 245–54.

18) Wang Y, Wu Y, Luo K, Liu Y, Zhou M, Yan S, Shi H, Cai Y (2013) The protective effects of selenium on cadmium-induced oxidative stress and apoptosis via mitochondria pathway in mice kidney. Food Chem Toxicol **58**, 61–7.

19) Kluck RM, Bossy-Wetzel E, Green DR, Newmeyer DD (1997) The release of cytochrome c from mitochondria: a primary site for Bcl-2 regulation of apoptosis. Science **275**, 1132–6.

20) Mohan S, Abdelwahab SI, Kamalidehghan B, Syam S, May KS, Harmal NS, Shafifiyaz N, Hadi AH, Hashim NM, Rahmani M, Taha MM, Cheah SC, Zajmi A (2012) Involvement of NF-κB and Bcl2/Bax signaling pathways in the apoptosis of MCF7 cells induced by a xanthone compound Pyranocycloartobiloxanthone A. Phytomedicine

19, 1007–15.

21) Liu B, Jian Z, Li Q, Li K, Wang Z, Liu L, Tang L, Yi X, Wang H, Li C, Gao T (2012) Baicalein protects human melanocytes from H_2O_2-induced apoptosis via inhibiting mitochondria-dependent caspase activation and the p38 MAPK pathway. Free Radic Biol Med **53**, 183–93.

22) Cui N, Li S, Zhao X, Zhang T, Zhang C, Yu L, Zhu Z, Xie K (2007) Expression of Bcl-2, Bax and Caspase-3 in nerve tissues of rats chronically exposed to 2,5-hexanedione. Neurochem Res **32**, 1566–72.

23) Sun Y, Lin Y, Li H, Liu J, Sheng X, Zhang W (2012) 2,5-Hexanedione induces human ovarian granulosa cell apoptosis through BCL-2, BAX, and CASPASE-3 signaling pathways. Arch Toxicol **86**, 205–15.

24) Wang Y, Sun Z, Qiu X, Li Y, Qin J, Han X (2009) Roles of Wnt/beta-catenin signaling in epithelial differentiation of mesenchymal stem cells. Biochem Biophys Res Commun **390**, 1309–14.

25) Carden MJ, Lee VM, Schlaepfer WW (1986) 2,5-Hexanedione neuropathy is associated with the covalent crosslinking of neurofilament proteins. Neurochem Pathol **5**, 25–35.

26) Lapadula DM, Suwita E, Abou-Donia MB (1988) Evidence for multiple mechanisms responsible for 2,5-hexanedione-induced neuropathy. Brain Res **458**, 123–31.

27) Wyllie AH (1997) Apoptosis: an overview. Br Med Bull **53**, 451–65.

28) Li XM, Han F, Liu DJ, Shi YX (2010) Single-prolonged stress induced mitochondrial-dependent apoptosis in hippocampus in the rat model of post-traumatic stress disorder. J Chem Neuroanat **40**, 248–55.

29) Mikhailov V, Mikhailova M, Degenhardt K, Venkatachalam MA, White E, Saikumar P (2003) Association of Bax and Bak homo-oligomers in mitochondria. Bax requirement for Bak reorganization and cytochrome c release. J Biol Chem **278**, 5367–76.

30) Zhang W, Feng H, Gao Y, Sun L, Wang J, Li Y, Wang C, Zhao L, Hu X, Sun H, Wei Y, Sun D (2013) Role of pigment epithelium-derived factor (PEDF) in arsenic-induced cell apoptosis of liver and brain in a rat model. Biol Trace Elem Res **151**, 269–76.

31) Cai BZ, Meng FY, Zhu SL, Zhao J, Liu JQ, Liu CJ, Chen N, Ye ML, Li ZY, Ai J, Lu YJ, Yang BF (2010) Arsenic trioxide induces the apoptosis in bone marrow mesenchymal stem cells by intracellular calcium signal and caspase-3 pathways. Toxicol Lett **193**, 173–8.

32) Merry DE, Korsmeyer SJ (1997) Bcl-2 gene family in the nervous system. Annu Rev Neurosci **20**, 245–67.

33) Wani BA, Ramamoorthy D, Rather MA, Arumugam N, Qazi AK, Majeed R, Hamid A, Ganie SA, Ganai BA, Anand R, Gupta AP (2013) Induction of apoptosis in human pancreatic MiaPaCa-2 cells through the loss of mitochondrial membrane potential ($\Delta\Psi$m) by Gentiana kurroo root extract and LC-ESI-MS analysis of its principal constituents. Phytomedicine **20**, 723–33.

34) Dwivedi N, Mehta A, Yadav A, Binukumar BK, Gill KD, Flora SJ (2011) MiADMSA reverses impaired mitochondrial energy metabolism and neuronal apoptotic cell death after arsenic exposure in rats. Toxicol Appl Pharmacol **256**, 241–8.

35) Wu CC, Yen CC, Lee I, Su CC, Tang FC, Chen KL, Su YC, Chen YW (2012) Involvement of oxidative stress-induced ERK/JNK activation in the Cu(2+)/pyrrolidine dithiocarbamate complex-triggered mitochondria-regulated apoptosis in pancreatic β-cells. Toxicol Lett **208**, 275–85.

36) Mishra DP, Pal R, Shaha C (2006) Changes in cytosolic Ca^{2+} levels regulate Bcl-xS and Bcl-xL expression in spermatogenic cells during apoptotic death. J Biol Chem **281**, 2133–43.

37) Zou C, Kou R, Gao Y, Xie K, Song F (2013) Activation of mitochondria-mediated apoptotic pathway in tri-ortho-cresyl phosphate-induced delayed neuropathy. Neurochem Int **62**, 965–72.

38) Roy S (2000) Caspases at the heart of the apoptotic cell death pathway. Chem Res Toxicol **13**, 961–2.

39) Li Q, Kobayashi M, Kawada T (2012) Mechanism of ziram-induced apoptosis in human T lymphocytes. Arch Toxicol **86**, 615–23.

40) Ramkumar KM, Manjula C, Elango B, Krishnamurthi K, Saravana Devi S, Rajaguru P (2013) In vitro cytotoxicity of Gymnema montanum in human leukaemia HL-60 cells; induction of apoptosis by mitochondrial membrane potential collapse. Cell Prolif **46**, 263–71.

41) Davila JC, Cezar GG, Thiede M, Strom S, Miki T, Trosko J (2004) Use and application of stem cells in toxicology. Toxicol Sci **79**, 214–23.

42) Zhang H, Wang ZZ (2008) Mechanisms that mediate stem cell self-renewal and differentiation. J Cell Biochem **103**, 709–18.

43) Kassem M, Abdallah BM (2008) Human bone-marrow-derived mesenchymal stem cells: biological characteristics and potential role in therapy of degenerative diseases. Cell Tissue Res **331**, 157–63.